Circumspect Exploration of Multidimensional Imbedded Shocks

Gino Moretti*
Polytechnic Institute of New York, Farmingdale, New York

Typical transonic flows with imbedded shocks are examined, using computed results from a two-dimensional, unsteady code with floating shock fitting. Physical evolutions from the initial formation of a shock to final steady states are described. Numerical problems related to such evolutions are pointed out, and suggestions are given for proper handling.

Introduction

NUMERICAL evaluations of transonic, steady, two-dimensional, inviscid flows have been attempted so far along two lines: 1) Assuming that the flow is rotational, and applying relaxation methods, and 2) using the nonlinear equations of motion for unsteady, rotational flows and working out a time-dependent evolution from an assumed initial flow towards an asymptotical steady state. The latter approach, while serving to produce steady state results, also provides a means of acquiring a better understanding of unsteady flows. Before attempting any numerical evaluation of complicated unsteady problems, however, it is necessary to become familiar with a number of basic flow patterns and their time evolutions, and to construct and validate numerical techniques that are consistent with their physical nature. In this context, the present paper examines certain phenomena related to the time-dependent evolution of imbedded shocks in transonic flows.

A Simple Problem and its Code

To fix ideas, consider the three typical steady-state situations shown in Fig. 1 (qualitatively). The first is a transonic flow, subsonic at infinity, with a supersonic bubble; the second is a transonic flow, supersonic at infinity, with a subsonic bubble; the third is a fully supersonic flow with an imbedded, oblique shock. The steady flow of Fig. 1c can be computed by integrating the steady equations of motion stepwise in the horizontal direction; therefore, no time-dependent technique is necessary, and the computation is actually one-dimensional. It is convenient, however, to examine the latter case in the general framework of time-dependent techniques, as a particular case of the problem which, for different free-stream Mach numbers, produces the patterns of Figs. 1a and 1b. In an unsteady flow, all three patterns sketched in Fig. 1 may occur at different evolutionary stages and a single computational program should be able to take care of them and of their unsteady neighbors automatically and accurately.

The problem poses a number of challenges to the numerical analyst. Some are related to the choice of initial conditions and to the treatment of boundary conditions; they will not be dealt with in the present paper. This study will be confined to a simple "boattail" geometry, similar to the one sketched in Fig. 1 (the wall extending to infinity in both directions horizontally), and will assume that such a wall has been set into motion from a state of rest in a gas at rest and brought rapidly to a constant cruising speed V_∞. An observer moving with the boattail may define a "steady" Mach number at infinity as $M_\infty = V_\infty/a_\infty$. The author will treat the imbedded shock as a discontinuity, in order to achieve maximum accuracy in a minimal computational time.[1] A question often asked is, "How can the formation of an imbedded shock be detected in an unsteady, multidimensional flow?" Despite widespread beliefs to the contrary, such a detection is easy and safe. Details about it will be given in full elsewhere, and here it will be assumed that the flow (and the computation) have already passed the initial phase and that an imbedded shock has formed and developed. It also will be assumed that a steady state is in the process of being reached. Finally, the author will disregard the case shown in Fig. 1b, since it resembles a blunt-body problem (with an impinging nonuniform but steady flow), and the blunt-body problem is well under control.

All of the following considerations are examined using a computer code, which performs the analysis outlined in the preceding description, for any prescribed value of M_∞, with an arbitrary choice of the boattail profile and of the acceleration of the boattail. The basic features of the code are described in Ref. 2, although some minor details have been altered in the version currently used. It is important to note that the code does not require external interventions.

In brief, the code performs a two-level integration of Euler's equations of motion at every grid point, using discretization procedures which, in a linearized analysis, assure second-order accuracy in space. The computational mesh is rather coarse (of the order of 30×20) and the mesh intervals (which are all different because of stretchings in both directions) are wide (the smallest being about 0.4 times the height of the boattail). The basic two-level scheme follows MacCormack's suggestion,[3] only because it is simple, not because of its alleged shock-capturing virtues (the equations of motion are not even written in divergence form). The shocks are fitted, using a floating technique that has been partially reported in Refs. 2 and 4. This entails not only ad hoc computations at shock points, both in front of and behind the discontinuity; it also requires special integration schemes for grid points whenever the standard scheme would operate on points located on both sides of a shock. There also are other special schemes used at boundary points and at certain points at which the flow is supersonic. The technique as a whole

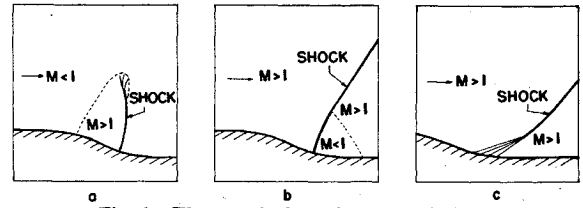

Fig. 1 Three typical steady transonic flows.

Presented at the AIAA 2nd Computation Fluid Dynamics Conference, Hartford, Conn., June 19-20, 1975 (no preprints, pp 10-16 bound volume Conference papers); submitted June 20, 1975; revision received Feb. 12, 1976. This research was sponsored by the Office of Naval Research under Contract N0014-75-C-0511, Project NR 061-135.

Index category: Subsonic and Transonic Flow.

*Professor, Department of Aerospace Engineering and Applied Mechanics. Associate Fellow AIAA.

seems to provide very accurate results, despite the coarseness of the mesh – a very important fact since the computational time is thus reduced to a minimum on a standard high-speed computer.[5]

Evolution of an Imbedded Shock towards a Steady Supercritical Pattern

The pattern of Fig. 1a is a typical steady pattern, which has been analyzed from a theoretical (qualitative) standpoint for more than a decade (see Ref. 6, Fig. 16 on p. 299). How such a pattern originates from an unsteady evolution is an extremely interesting problem and, in the author's opinion, its appearance in a numerical computation is a demonstration of what should be expected from a well-working program (that is, a program capable of being physically meaningful at every computational step). In Fig. 2a, a number of different locations of an imbedded shock are shown, starting from its formation, which occurs shortly after the wall has been set into motion from a state of rest in a gas at rest, and brought rapidly to a constant cruising speed ($M_\infty = 0.8$). It may be noted that the shock picks up strength and increases in length. A measure of the strength of the shock is given by the normal Mach number relative to it, M_n, which is shown in Fig. 3.

Note that, at its formation and during the early stages of its evolution, the shock is not normal to the wall, and M_n is practically equal to 1 along the whole shock (steps 50 and 100 in Figs. 2a and 3a). Once the shock becomes normal to the wall, it gathers strength rapidly in the vicinity of the wall, where the relative normal Mach number grows to supersonic values. In the vicinity of the wall, the absolute velocity of the shock tends to vanish, and the shock practically locks into a fixed position rather early in the total evolution process (see, in Fig. 2a, how little the wall shock point advances between step 150 and step 680, as compared with the advance between step 50 and step 150). At a greater distance from the wall, however, M_n tends to remain very close to 1 for a much longer time.

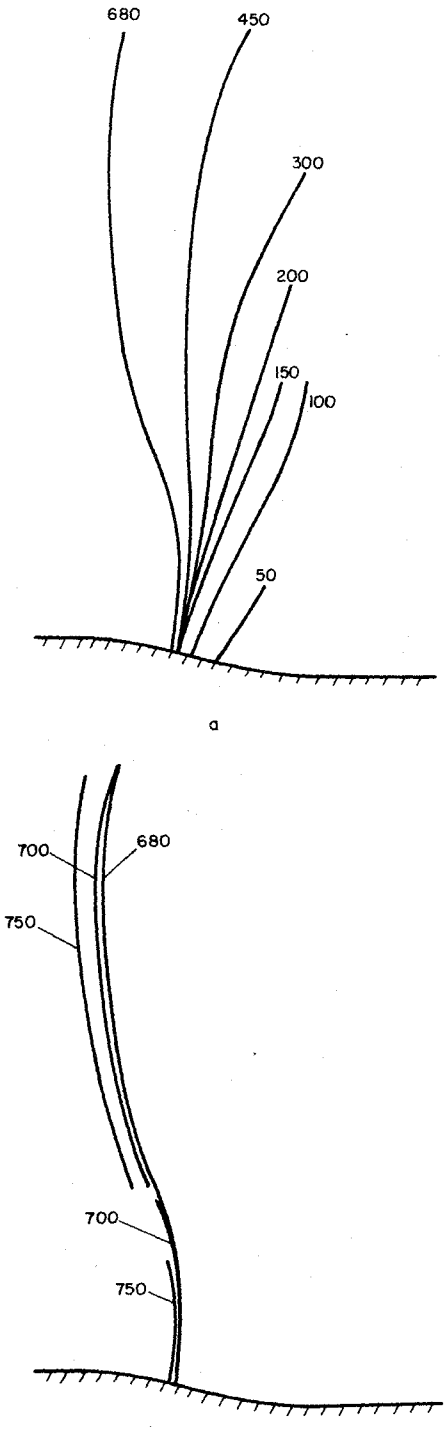

Fig. 2 Evolution of an imbedded shock, $M_\infty = 0.8$ (numbers denote computational steps).

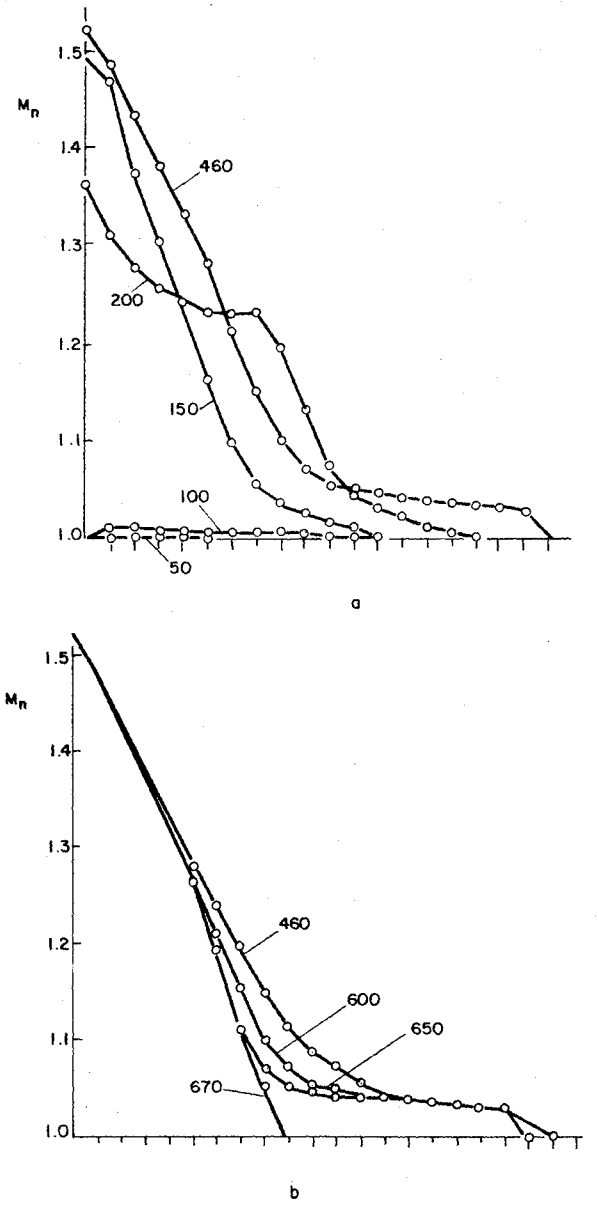

Fig. 3 Normal Mach number at computed locations along the shock, $M_\infty = 0.8$.

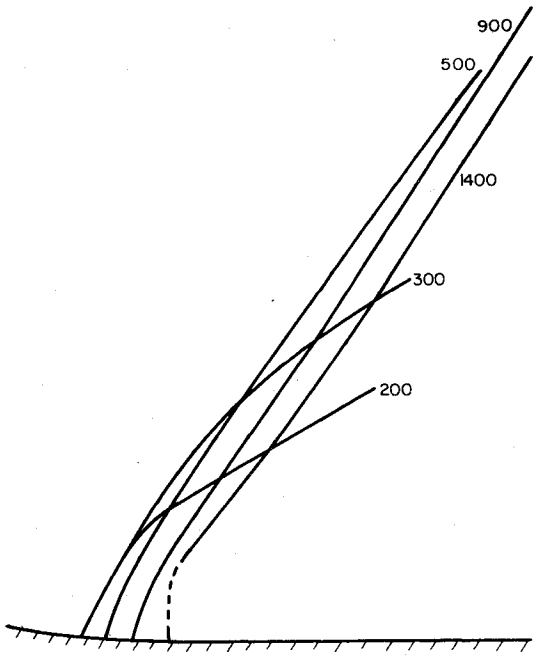

Fig. 4 Evolution of an imbedded shock $M_\infty = 1.1$.

The upper part of the shock essentially continues to advance as an unsteady characteristic in a subsonic flow.

As a consequence, somewhere in the vicinity of the upper part of the supersonic bubble, the shock becomes more and more oblique with respect to the streamlines M_n becomes locally equal to 1, and the shock rips apart. The upper part moves away, almost as an unsteady characteristic, and eventually disappears. The lower part shrinks to a shorter length. This part of the shock evolution is shown in Fig. 2b, and its distribution of values of M_n are shown in Fig. 3b. Note that the ripping process is started by a decay of M_n in the middle of the shock, and that such decay is not produced by changes in the surrounding flow, but by changes in the shock geometry.

A similar but opposite evolution takes place when the stream is supersonic throughout (Fig. 1c). In Fig. 4, successive locations of the imbedded shock are shown for the case in which the cruising Mach number at infinity equals 1.1. It appears that now it is the lower part of the shock which has to separate from the rest (all but locked in a steady configuration) and to be wiped away with the flow.

Considerations about Stability of an Imbedded Shock Computation

In seeing a set of results such as those presented in Figs. 2 and 4, one naturally is led to inquire about their accuracy. There are, of course, no general rules to evaluate the accuracy of a computation dealing with nonlinear problems of which no exact solution is available. There are, however, "confidence builders." One is that, by and large, the computation is stable. For years it has been believed that shock-fitting techniques are numerically unstable.[6] A number of arguments have been forwarded to support such a belief; sometimes, the words "nonlinear instability" have been used for lack of an explanation. Very careful analysis of details of a computation eventually will show that instabilities are just the ultimate catastrophy of a program that generates unrealistic perturbations, many of which may remain confined within finite limits, and even be wiped out by much stronger physical variations. Wiggles that are clearly dependent on the mesh should be watched as the most significant tell-tale of an unrealistic computational technique. Now, in a two-dimensional, time-dependent problem, many elements

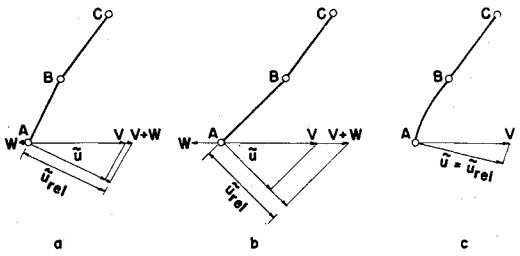

Fig. 5 Numerical instability at the end-point of a shock.

act simultaneously to generate the values needed in updating, and some of them may be coded in such a way that their interaction tends to amplify errors. A pragmatic discussion of this subject largely exceeds the limits of the present paper. In order to give an idea of the problem, let us consider what happens if a point A is to be computed as the end-point of a shock in which the relative normal Mach number M_n is reasonably assumed to be 1 (Fig. 5a). Let B be the next computed point on the shock, and let us assume that B is computed properly and does not move. Let V be the incoming flow velocity at A, and $\tilde{u}$ its component normal to the shock. The normal Mach number $\tilde{u}/a$ may to be less than 1; therefore, in order to enforce the condition $M_n = 1$, a shock velocity component W must be added, as shown in Fig. 5a, so that $\tilde{u}_{\text{rel}} = \neq$. This forces A to move to the left with a velocity W; at the next computational step (Fig. 5b), and with the same impinging velocity V, $\tilde{u}$ is smaller; consequently, W must be larger, and the shock configuration is clearly unstable. Where does the computation fail? In the previous argument, it is simplisticly assumed that the slope of the shock at A is the slope of the segment AB. In the shock geometry shown in Fig. 5c, however, which is compatible with the locations of A,B, and C given in Fig. 5a, the normal to the shock at A allows M_n to be locally equal to 1, with $W=0$; such configuration, therefore, is stable.

The Tip of an Imbedded Shock in a Supercritical Flow

The example clearly shows how a hard-to-evaluate geometrical parameter can influence, and perhaps produce, catastrophy in an otherwise well-behaved computation. Fortunately, difficulties of this nature do not appear too frequently. In the evolution shown in Fig. 2, the initial shock tends to steepen at the wall because of a strong piling up of compression waves behind the shock at a short distance from the wall; the evolution is stable and, in a short time, the shock locks in a configuration normal to the wall. On the other hand, the tip of the shock moves rapidly in a region of almost unperturbed flow and small inaccuracies are harmless. In the case of Fig. 1b, as in any blunt-body problem, the final steady shock extends to infinity and there is no tip to compute. The final evolution of the case of Fig. 1a, after the partins of the shock and until a steady state is reached, and its counterpart in the case of Fig. 1c, are harder to keep under control. Not only is the geometry of the shock a challenge to discretization, as shown previously, but also the environment of the shock is difficult. It must be noted that the nature of the steady flow is totally different from the nature of its unsteady buildup. An unsteady flow always is hyperbolic; the domain of dependence of a point is a cone in space-time, a circle in space. In the supersonic part of a steady flow, the domain of dependence is an angle. In the case of Fig. 1c, it is customary to say that the imbedded steady shock is formed by coalescence of pressure waves proceeding from the wall, and that the shock begins where such waves would overlap. Similarly, in the case of Fig. 1a, the steady shock begins in the middle of the flowfield, produced by a similar coalescence of pressure waves in a supersonic flow in which the upper part of the shock is fully imbedded. It should be clear that, as the initial

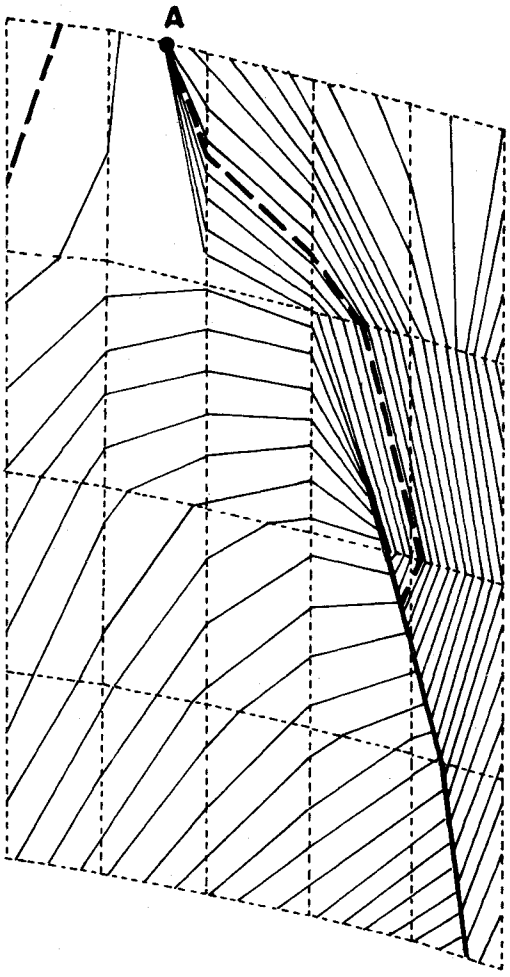

Fig. 6 Isobar pattern around the tip of the shock, $M_\infty = 0.8$.

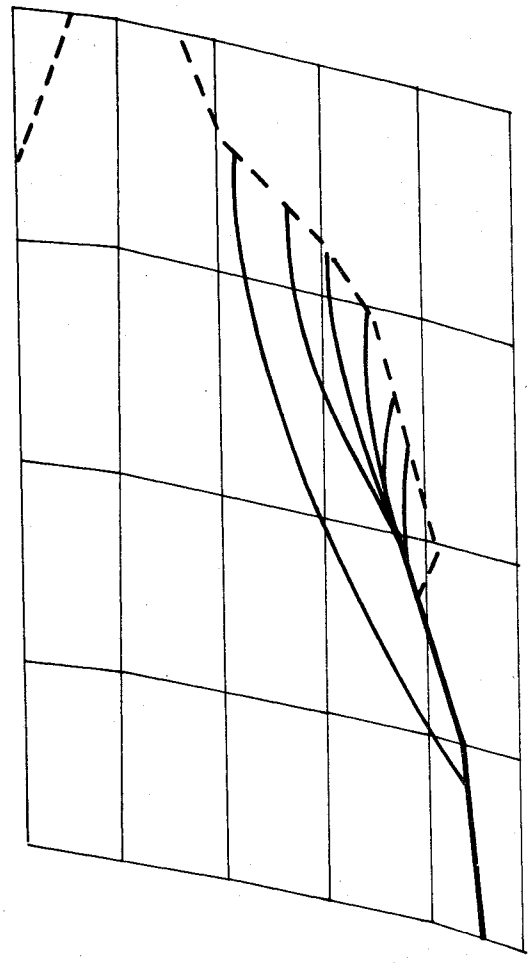

Fig. 7 Down-running steady characteristics as computed from the unsteady pattern of Fig. 6.

point in the shock of Fig. 1c is the crucial element in the determination of the geometry of the imbedded shock, so is the upper endpoint of the shock in Fig. 1a. In neither case is one allowed to guess the position of the endpoint, even partially (for example, by assuming that it lies on a certain grid line); the point must be let free to move to its proper location, even if such freedom entails a certain amount of additional programming!

Consider Fig. 6, which depicts the computed situation near the tip of the shock (for the case of Fig. 1a) shortly before a steady state is reached. In the figure, one sees part of the computational grid (dotted lines), a pattern of isobars obtained by linear interpolations of computed pressure values at grid points and shock points (light solid lines), and also part of the shock (heavy solid line). The broken heavy line is the boundary of the supersonic bubble. Note that the flow near the upper grid line is still far from being steady. There is actually a point A, representing the bottom of the weak unsteady shock, which is in the process of moving away against the incoming flow at a relatively high speed. The supersonic pattern in the two bottom grid rows is steady and it has remained unchanged, for all practical purposes, for a long time. A test of total temperature, as computed from the local Mach numbers, vs the total temperature of the steady flow (which is exactly 1.128), shows local deviations not larger than 0.0002. The amount of detail available, despite the coarseness of the grid, is impressive. Not only does the computed flow appear free of any mesh-dependent wiggles; the curving of pressure waves near the top of the supersonic bubble and their incipient coalescence towards the end point of the shock is typical of what we may expect in a steady-state configuration. Drawing a pattern of steady characteristics is much harder, since the local Mach number is very close to 1 and the slopes of the characteristics change very rapidly. An attempt is shown in Fig. 7; the trend is definitively correct.

Needs for Special Codings of Certain Derivatives

Such a pattern suggests that the numical domain of dependence for points in the supersonic region, at the level of the tip of the shock and above, should be essentially backwards and upwards with respect to the computed point. It is easy to see that an overall second-order-accurate integration scheme is obtained if the usual MacCormack formula is used in one direction, Y, whereas the X derivatives at a point ($X=n\Delta X$, $Y=m\Delta Y$) are defined at the predictor stage as

$$f_{x_{(n,m)}} \approx (1/\Delta x)\,(2f_{n,m} - 3f_{n-1,m} + f_{n-2,m})$$

and at the corrector stage as

$$f_{x_{(n,m)}} \approx (1/\Delta x)\,(f_{n,m} - f_{n-1,m})$$

The former can be interpreted as

$$f_{x_{(n,m)}} \approx f_{x_{(n-1,m)}} + \Delta x \cdot f_{xx_{(n-1,m)}}$$

with $f_{x_{(n-1,m)}}$ approximated by a forward difference, whereas the latter deals with a backward difference. The author has used schemes of this kind on many occasions, typically at wall points and at boundary points. In the present context, such schemes provide interesting domains of dependence (varying, of course, according to the nature of the environment), which remain consistent with the domain of dependence of the un-

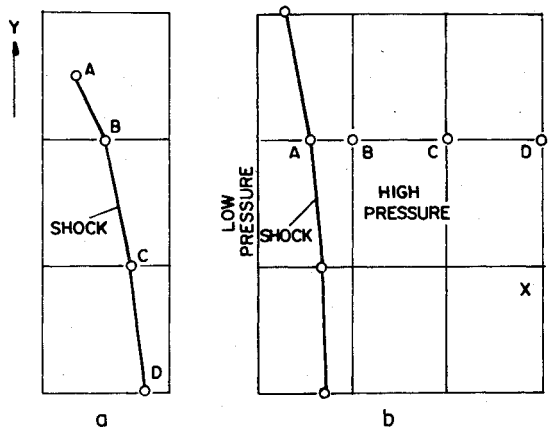

Fig. 8 To illustrate discretization at points A and B.

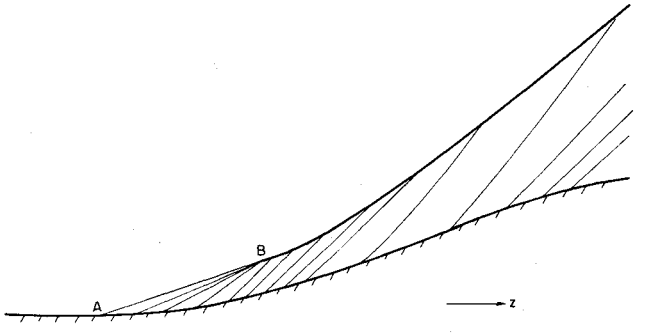

Fig. 9 A shock imbedded in a steady, supersonic flow, $M_\infty = 3$.

steady flow equations, but also overlap the domain of dependence of the steady flow characteristic pattern. It seems that such an overlapping is needed to maintain accuracy and stability when the unsteady flow becomes steady. The results indeed are very encouraging.

The argument related to Fig. 5 and the trend of the steady characteristics suggest that a prudent use of a preferential direction also should be made in evaluating the slope of the shock near its end point. There is a striking resemblance between the situation at points A,B on a shock (Fig. 8a) and at points A,B on a grid line (Fig. 8b). In both cases, A is a terminal point; derivatives at A can be approximated only by assuming information on one side – in Fig. 8a, from points such as $B,C,\ldots$ on the shock; in Fig. 8b, from points such as $B,C,\ldots$ on the high-pressure side of the grid line. Derivatives at B must be approximated by using information at $B,C,\ldots$*but also at* A. If point A were not used, the computation at B would remain totally uncoupled from the flow values at A; it has been observed instead, that the slope of the shock at A(Fig. 8a) must influence the rest of the shock geometry; similarly, signals from the back of the shock (point A in Fig. 8b) must be allowed to reach and influence neighboring downstream points. The following formulas satisfy the previous conditions. Let

$$d=\Delta Y \qquad \epsilon=(Y_A-Y_B)/d \text{ in Fig. 8a}$$

$$d=-\Delta X \qquad \epsilon=(X_A-X_B/d \text{ in Fig. 8b}$$

$$\delta_1=(1-\epsilon)/(1+\epsilon) \qquad \delta_2=\epsilon\delta_1$$

Then, f being any function

$$f'=(1/d)\,[1.5f_A-2\epsilon f_B-(2-2.5\epsilon)f_C+0.51(1-\epsilon)f_D] \quad (1)$$

approximates $\partial f/\partial Y$ at A and $\partial f/\partial X$ at A in Fig. 8a and Fig. 8b, respectively. This expression is only first-order-accurate, but is not jumping when point A crosses a grid line. In order to approximate $\partial f/\partial Y$ at B in Fig. 8a and $\partial f/\partial X$ at B in Fig. 8b, the following expression, accurate to the second order, is used:

$$(1/d)\,[f_A-(1-\delta_2)f_B-\delta_2 f_C]+\delta_1 f'$$

with f' as defined in Eq. (1).

More Tests for Stability

Additional tests for stability were first conducted in an "aseptic" environment. A steady supersonic flow, uniform at infinity and containing an imbedded shock, was computed about the wall geometry of Fig. 9 by a one-dimensional code marching in the horizontal direction. Results from this code were used as initial data for a two-dimensional, unsteady code with an imbedded shock treated by a floating technique. The wall geometry has a discontinuous curvature at a point A; therefore, the imbedded shock originates at a point B along the characteristic issuing from A, and the flow in front of it is uniform. This simplifies the shock equations and the treatment of the endpoint of the shock B. Unfortunately, the effect of a discontinuous wall curvature is a sudden increase in the shock normal Mach number at B. Some numerical trouble may be expected, if the normal Mach number is forced to be 1 at B and there are no provisions in the code for an infinite slope of the Mach number distribution curve along the shock. It was found, however, that as long as the numerical domain of dependence of the points between A and B does not allow feedback of numerical disturbances generated immediately downwards of B into the A-B region, the results are stable, and a minor local departure (at B) of the results of the unsteady code from the results of the steady code does not affect the rest of the computation. The shock as computed by the unsteady flow code, lies on top of the steady curve shown in Fig. 9. The pressure distribution behind the shock shows some difference only in the immediate vicinity of B. Note that the two-dimensional unsteady code works on a much coarser mesh than does the one-dimensional, steady code; in the vicinity of B, the gradients are very steep, and one is practically asking the program to compute zero time derivatives as combinations of infinite space derivatives in both space directions. As soon as the unsteady computation is started from the initial steady data, some minor oscillation appears in the vicinity of B, but it is carried away long the shock, a behavior that attests of the physical soundness of the code. Success in this case encourages the hope for even better results in problems in which the wall curvature is continuous.

A Point to be Further Explored

In problems such as the ones shown in Figs. 1a and 1c, care must be taken in determining the conditions in front of the endpoint of the shock, since the flow is no longer uniform. In the examples treated so far, simple linear interpolations between neighborhod grid points were sufficient; nevertheless, it is known experimentally that, in the case of Fig. 1a, the environment of the tip of the shock is very sensitive to any external perturbation. Instabilities may occur physically thereabout, if wavelets propagate through a generally steady flow. Stable numerical results might conceal unwanted dampings due to truncation errors, and the subject requires more numerical experimentation.

Interplays of Different Effects and Some Suggestions for their Analysis

In conclusion of this brief report of analysis, the fact should be emphasized that totally different effects are tightly interwoven in a two-dimensional, unsteady calculation, because it so happens in nature. Such a calculation, thus, is by far more difficult to understand and to conduct properly than any one-dimensional calculation. From the enormous stack of

information available at every step and at every point, a certain number of parameters must be singled out and their patterns, in space and time, must be analyzed carefully. In Ref. 2, it has been pointed out that drawing isobars, either over the computation region at a given time (as in Fig. 6), or in time over a fixed line (this shows the propagation of waves) is very important. The shape of the shock is interesting and significant, but it is not a very sensitive element; trouble may have started long before the shock begins showing instability. Of the two Cartesian components of the unit vector normal to the shock at each point, one is a very sensitive parameter and must be watched; this is true also for the normal relative Mach number. Minor changes in M_n (for example, from 1.01 to 1.02) are associated with sizable changes in pressure ratio across the shock (from 1.023 to 1.047, respectively). In a situation such as in the upper part of Fig. 6, too high pressure values behind the upper part of the parted shock tend to flatten the supersonic bubble, inducing high pressures in front of the end point of the lower shock, and influencing its geometry catastrophically.

By far, the most sensitive parameter is the shock acceleration. The equation used to compute it is the most complicated in the program, since it includes the simultaneous effects of variable upwind parameters, variable shock geometry, Rankine-Hugoniot conditions, and a characteristic equation behind the shock. All of the terms in the equation, however, can be grouped into three categories, expressing three well-differentiated physical effects: 1) the effects of variable upwind parameters and variable shock geometry; 2) the effects of space variations of downwind parameters along the shock; and 3) the pull-push effects of space variations of downwind parameters in a direction normal to the shock. Each of the groups should be followed closely, particularly in the initial phases of shock formation and in the vicinity of a steady state.

In the latter case, obviously, the effects under item 1 of the preceding paragraph should vanish. In fact, the upwind values, which belong to a supersonic region, are the first to be stabilized; if this does not happen, it probably is because inaccuracies from downstream find a way of creeping into the upstream flow, probably by circumventing the supersonic bubble. The effects under items 2 and 3 never vanish. In a one-dimensional nozzle, the shock locks into place, because the pressure gradient downstream of the shock, which tends to push the shock upstream, is compensated by a divergent channel area change, which tends to push the shock downstream (remember that this is producing a stable configuration; the opposite effects in a convergent channel leads to a mathematically plausible, but physically unstable, shock location). In a similar way, the effects under items 2 and 3 must reach equal and opposite values in a steady, two-dimensional shock configuration. It is advisable to output them at every level of every step, and for every shock point, together with the shock acceleration, and to use them as indicators of yet undetected numerical inaccuracies.

References

[1]Moretti, G., "On the Matter of Shock Fitting," *Proceedings of the Fourth International Conference of Numerical Methods in Fluid Dynamics*, Boulder, Colo. June 1974, pp. 287-292.

[2]Moretti, G., "Floating Shock Fitting Technique for Imbedded Shocks in Unsteady Multidimensional Flows," *Proceedings of the 1974 Heat Transfer and Fluid Mechanics Institute,* Stanford University Press, Stanford, Calif., 1974, pp. 184-201.

[3]MacCormack, R.W., "The Effect of Viscosity in Hypervelocity Impact Cratering," Paper 69-354, *Presented at the AIAA 7th Aerospace Sciences Meeting*, New York, 1969.

[4]Moretti, G., "Experiments in Multi-Dimensional Floating Shock-Fitting," PIBAL Rept. 73-18, Polytechnic Institue of Brooklyn, Aug. 1973.

[5]Ferrari, C. and Tricomi, F.G., *Transonic Aerodynamics*, Academic Press, Inc., New York, 1968.

[6]Nieuwland, G.Y. and Spee, B.M., "Transonic Airfoils: Recent Developments in Theory, Experiment, and Design,"*Annual Review of Fluid Mechanics*, Vol. 5, 1973, pp. 119-150.